Tunneling magnetoresistance in Si nanowires

2016 New J. Phys. 18 113024

(http://iopscience.iop.org/1367-2630/18/11/113024)

New Journal of Physics
The open access journal at the forefront of physics

Deutsche Physikalische Gesellschaft DPG
IOP Institute of Physics

Published in partnership with: Deutsche Physikalische Gesellschaft and the Institute of Physics

OPEN ACCESS

RECEIVED
21 July 2016

REVISED
25 September 2016

ACCEPTED FOR PUBLICATION
20 October 2016

PUBLISHED
9 November 2016

PAPER

Tunneling magnetoresistance in Si nanowires

E Montes[1], **I Rungger**[2,3], **S Sanvito**[2] **and U Schwingenschlögl**[1]

[1] King Abdullah University of Science and Technology (KAUST), Physical Science and Engineering Division (PSE), Thuwal 23955-6900, Saudi Arabia
[2] School of Physics and CRANN, Trinity College, Dublin 2, Ireland
[3] Materials Division, National Physical Laboratory, Teddington, TW11 0LW, UK

E-mail: udo.schwingenschlogl@kaust.edu.sa

Keywords: nanowire, magnetoresistance, quantum transport

Abstract

We investigate the tunneling magnetoresistance of small diameter semiconducting Si nanowires attached to ferromagnetic Fe electrodes, using first principles density functional theory combined with the non-equilibrium Green's functions method for quantum transport. Silicon nanowires represent an interesting platform for spin devices. They are compatible with mature silicon technology and their intrinsic electronic properties can be controlled by modifying the diameter and length. Here we systematically study the spin transport properties for neutral nanowires and both *n* and *p* doping conditions. We find a substantial low bias magnetoresistance for the neutral case, which halves for an applied voltage of about 0.35 V and persists up to 1 V. Doping in general decreases the magnetoresistance, as soon as the conductance is no longer dominated by tunneling.

1. Introduction

Magnetic tunneling junctions (MTJs) are the basic elements in modern magnetic sensors and magnetic data storage systems [1]. They are formed by sandwiching a thin insulating tunnel barrier between two ferromagnetic electrodes. If the insulating layer is thick enough, electrons will tunnel between the ferromagnets, and when the mutual alignment of the magnetization vectors of the electrodes changes from antiparallel to parallel there is a drop in the resistance of the junction. This is known as the tunneling magnetoresistance (TMR) effect [2].

TMR was observed for the first time in a Co/Ge/Fe junction, where the change in tunneling current was found to be nearly 14% at 4.2 K [3]. It is also established that the magnitude of the effect is related to the spin polarization of the electrodes, namely to the spin imbalance of the current carried in the ferromagnets [3, 4]. This prediction held true for a vast range of subsequent experiments, all using amorphous tunnel barriers as spacer between the electrodes [2, 5]. At the same time it stimulated the use of highly spin-polarized electrodes, and in fact the maximum TMR values are expected for half-metals, namely for ferromagnets presenting a band gap at the Fermi energy (E_F) in only one of the two spin sub-bands [6]. However, usually the half-metallic state depends sensitively on the materials purity, and typically this is limited in real devices. For this reason there are not many examples of high-performing MTJs made of half-metals.

Fortunately, the problem of the spin polarization of the electrodes can be circumvented by an appropriate tunnel barrier choice. In fact, in crystalline insulators the exponential decay of the wave function of the tunneling electrons across the barrier depends on the symmetry of the tunneling states. Thus, one can engineer junctions in which only one spin type is transmitted across the barrier with high efficiency, while the other is almost completely reflected. For instance, this is the case for Fe/MgO/Fe grown along the (001) direction [7, 8], a system that displays giant TMR [9, 10]. This aspect of TMR inspired a significant number of studies aiming at designing novel junctions with high-performing and sometimes multifunctional tunnel barriers. These, for instance, include ferroelectric materials [11–14], ferromagnetic semiconductors [15, 16] and two-dimensional layered compounds [17, 18]. There are also proposals for unconventional magnetoresistance at the surface of topological insulators [19]. Recently, there have been attempts to perform magnetoresistance experiments with semiconductor nanowires [20], as quantum confinement can be a tool to manipulate spin scattering.

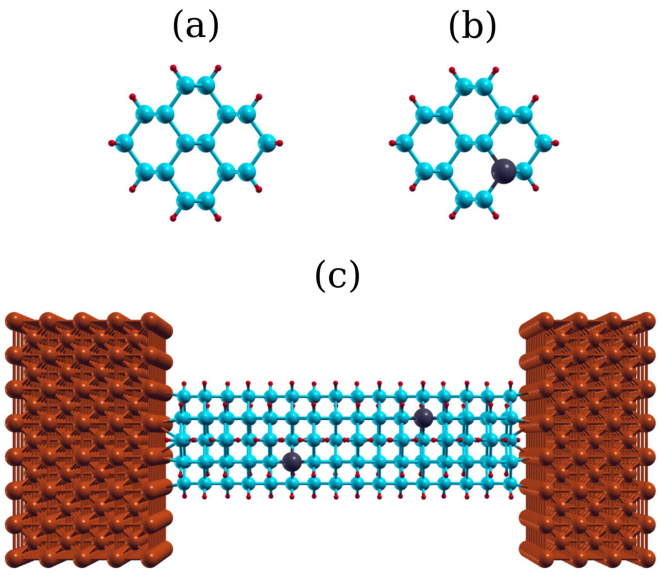

Figure 1. Cross sections of (a) a pristine and (b) a doped ⟨110⟩-oriented SiNW. Blue and red spheres represent Si and H atoms, respectively. The dopant atoms are shown in gray. (c) Geometry of the MTJ, comprising a SiNW sandwiched between two Fe ⟨111⟩-oriented electrodes.

Si nanowires (SiNWs) are attractive candidates for spintronics applications, since the spin coherence in Si has been demonstrated to be extremely long [21]. SiNWs are compatible with conventional Si technology and have been adapted in a variety of nanoscale devices, such as transistors [22], photodetectors [23] and solar cells [24]. The ability to control their diameter, composition and length makes them a desirable platform for spintronics studies [25], and previous work has demonstrated that the tunneling properties depend on the structural parameters [26]. In addition, the inclusion of *n* and *p* dopants has shown to modify the conductance [27].

Here we investigate Fe/SiNW/Fe MTJs having a SiNW as spacer and Fe magnetic electrodes. We first characterize the properties of the Fe/SiNW interface and then analyze the magneto transport by calculating the transmission coefficient at zero and finite applied bias. We compute the current–voltage (*I*–*V*) characteristics and evaluate the bias-dependent TMR. Then we study the influence of *n* and *p* dopants on the magnetic properties, the *I*–*V* characteristics and the TMR of the nanowire, and compare the magneto transport for the two doping situations.

2. Methodology

The SiNWs have been generated without considering surface reconstruction by applying Wulff's law for minimal free energy equilibrium [28], where a cylindrical shape with a core that retains the diamond structure is the most stable configuration [29]. In order to ensure chemical stability, dangling bonds have been passivated with H. The growth direction has been chosen to be ⟨110⟩, which was reported to have the smallest tunneling decay coefficient among all possible orientations [26, 30] and therefore is the orientation able to support the largest conductance. Figure 1(a) displays the cross section of a SiNW grown in the ⟨110⟩ direction with diameter $D = 1.0$ nm, where the blue and red spheres represent Si and H atoms, respectively. Single impurities dope the SiNW and are placed on its surface, since these positions have the lowest overall formation energy [31, 32]. In figure 1(b) we show the cross section of a doped SiNW, where the gray spheres correspond to P and B atoms in the case of *n* and *p* doping, respectively.

The structures are fully relaxed by density functional theory, using the local-orbital code SIESTA [33], until the forces on all the atoms are less than 0.04 eV Å^{-1}. A double zeta basis set with polarization functions is used for all the simulations. Core electrons are described by norm-conserving Troullier–Martins pseudopotentials [34] and the exchange-correlation functional is approximated by the Perdew–Burke–Ernzerhof [35] parameterization of the generalized gradient approximation. The real-space grid cutoff has a corresponding cutoff energy of 500 Ry and an electronic temperature of 300 K is used for all the calculations.

Transport calculations are performed using the SMEAGOL code, which combines density functional theory with the non-equilibrium Green's function method for electron transport [36–38]. Semi-infinite electrodes are connected to a central scattering region by means of energy, *E*, and spin-dependent self-energies, $\Sigma^{\sigma}_{\mathrm{L,R}}(E)$. The

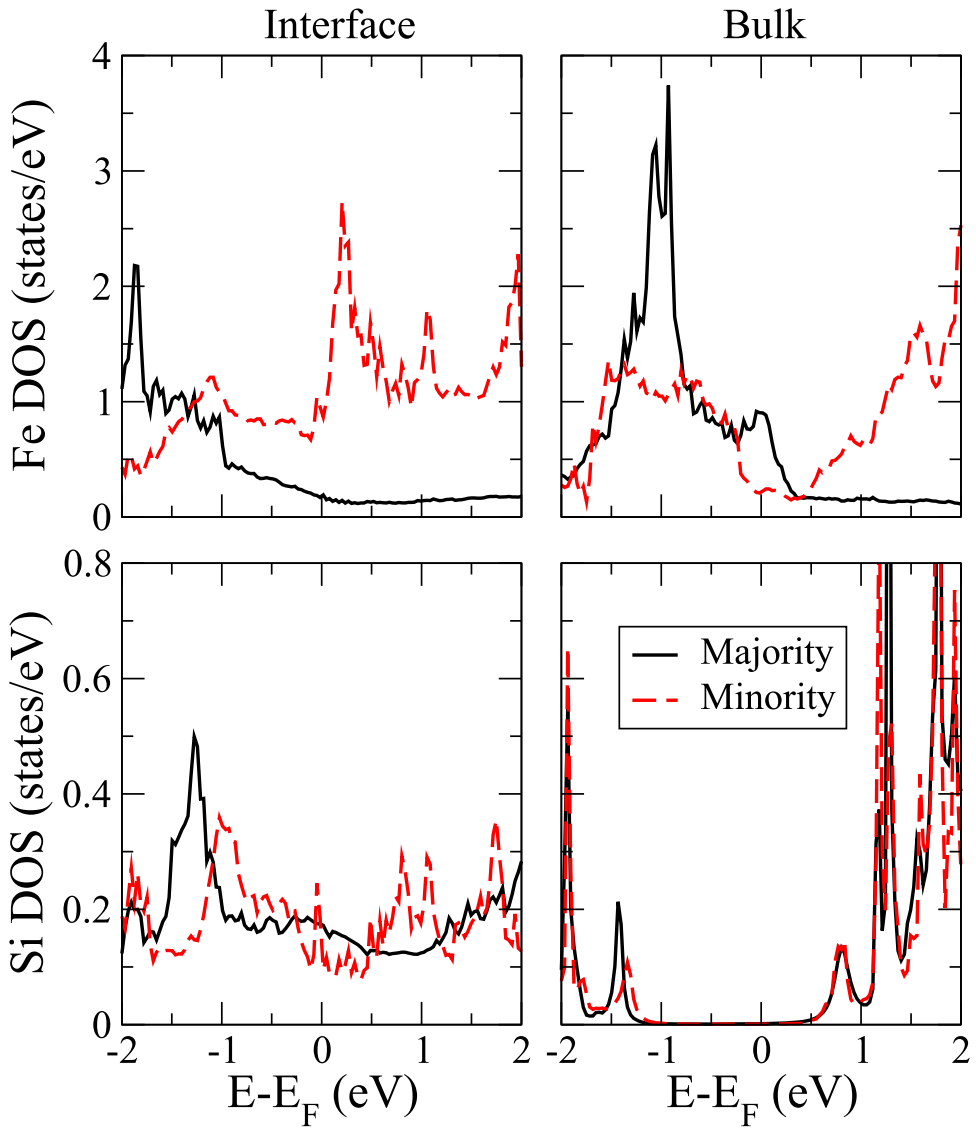

Figure 2. Spin-dependent density of states projected on Fe and Si. Left panels are for atoms located at the Fe/Si interface, while right panels are for atoms in the bulk, respectively, in the middle of one electrode and in the SiNW.

spin-dependent transmission coefficient, T^{σ}, is then calculated as

$$T^{\sigma}(E) = \mathrm{Tr}\,[G_{\mathrm{C}}^{\sigma}(E)\Gamma_{\mathrm{L}}^{\sigma}(E)G_{\mathrm{C}}^{\sigma\dagger}(E)\Gamma_{\mathrm{R}}^{\sigma}(E)], \tag{1}$$

where σ is the spin index ($\sigma = \uparrow, \downarrow$), $G_{\mathrm{C}}^{\sigma}(E)$ is the retarded Green's function of the scattering region and $\Gamma_{\mathrm{L,R}}^{\sigma}(E) = \mathrm{i}[\Sigma_{\mathrm{L,R}}^{\sigma}(E) - \Sigma_{\mathrm{L,R}}^{\sigma\,\dagger}(E)]$. The transmission coefficient is self-consistently evaluated at finite bias, V, and integrated to calculate the spin current,

$$I^{\sigma}(V) = \frac{e}{h}\int [f_{\mathrm{L}} - f_{\mathrm{R}}]\,T^{\sigma}(E,\,V)\mathrm{d}E, \tag{2}$$

where e is the electron charge, h the Planck constant, $f_{\mathrm{L,R}}$ the Fermi function $f_{\mathrm{L,R}} = 1/\{\exp[(E - \mu_{\mathrm{L,R}})/k_B T] + 1\}$, and μ_{L} (μ_{R}) the electrochemical potential of the left-hand (right-hand) side electrode ($\mu_{\mathrm{L}} - \mu_{\mathrm{R}} = eV$). The total current is then given by $I = I^{\uparrow} + I^{\downarrow}$ and the TMR is calculated with the 'optimistic' definition

$$\mathrm{TMR} = \frac{I_{\mathrm{P}} - I_{\mathrm{AP}}}{I_{\mathrm{AP}}}, \tag{3}$$

where I_{P} (I_{AP}) is the current that flows through the junction for parallel (anti-parallel) alignment of the magnetizations of the two electrodes. We note that our methodology is valid only for materials with long spin coherence, such as Si. The MTJ under study is presented in figure 1(c), and consists of a SiNW (pristine or doped) placed between two Fe ⟨111⟩-oriented electrodes. The SiNW has a total length of $l = 30.7$ Å and the

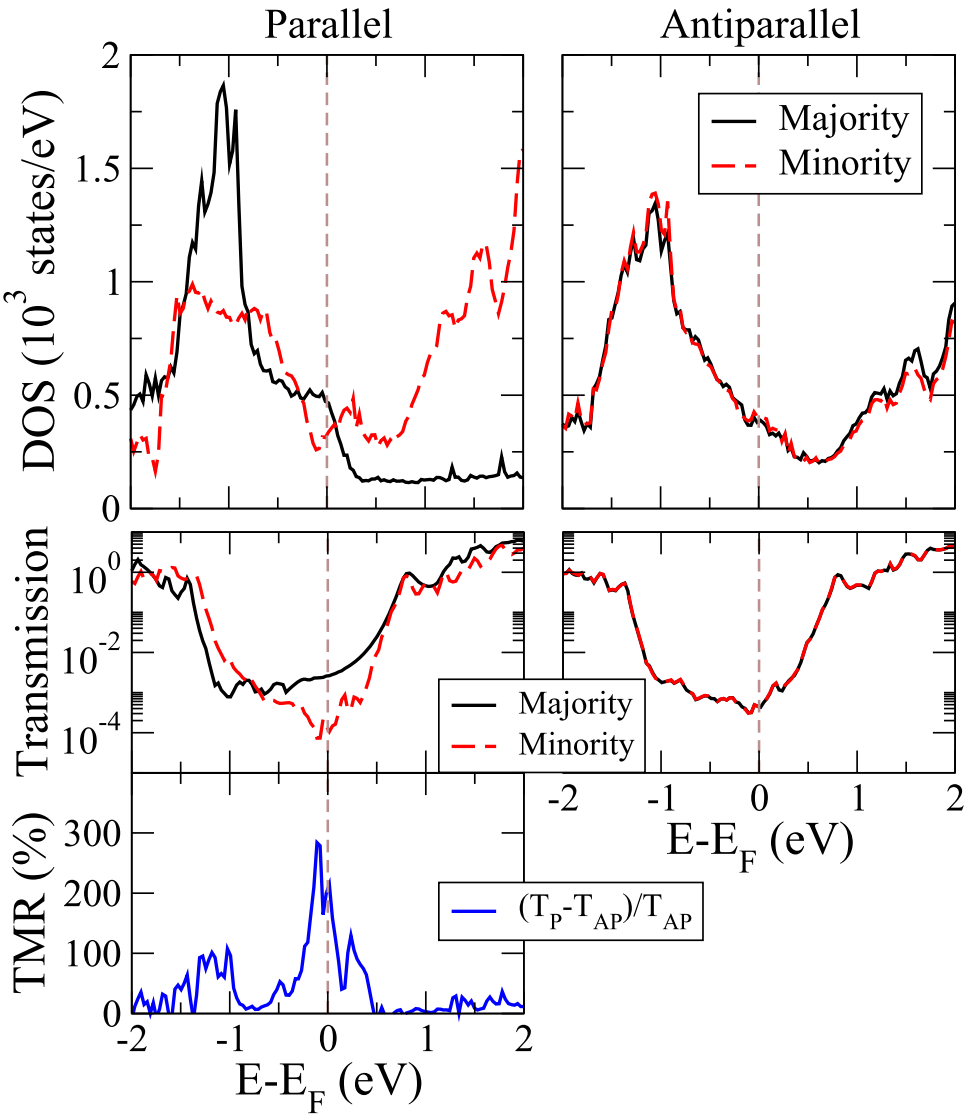

Figure 3. The upper panels present the spin-dependent total DOS and the middle panels the transmission coefficient of the MTJ pictured in figure 1. The left panels are for the parallel configuration and the right panels for the antiparallel configuration. The lower panel shows the TMR ratio as a function of energy.

dopant atoms are distributed equidistantly through the scattering region in positions that have equivalent formation energy.

3. Results and discussions

We divide the results into two parts. Firstly, we characterize the Fe/SiNW interface and discuss the TMR effect of a pristine SiNW-based MTJ. Secondly, we analyze the effect of *n* and *p* doping on the TMR.

3.1. Pristine SiNW

In figure 2 we present the spin-dependent density of states (DOS) projected on the Fe and Si atoms for both bulk-like positions (far away from the interface) and at the Fe/Si interface. The DOS of the Fe atoms placed in the middle of the electrodes behaves, as expected, as that of bulk Fe. There is a predominant majority d state contribution at E_F in virtue of a valley in the minority DOS due to d orbital splitting. Similarly, the DOS associated with Si atoms in the middle of the SiNW is consistent with the electronic structure of the nanowire in isolation. The DOS is that of a semiconductor with a spin-independent band gap of about 1.5 eV, in agreement with literature (considering this particular diameter) [26]. From this electronic structure one should expect a tunneling conductance.

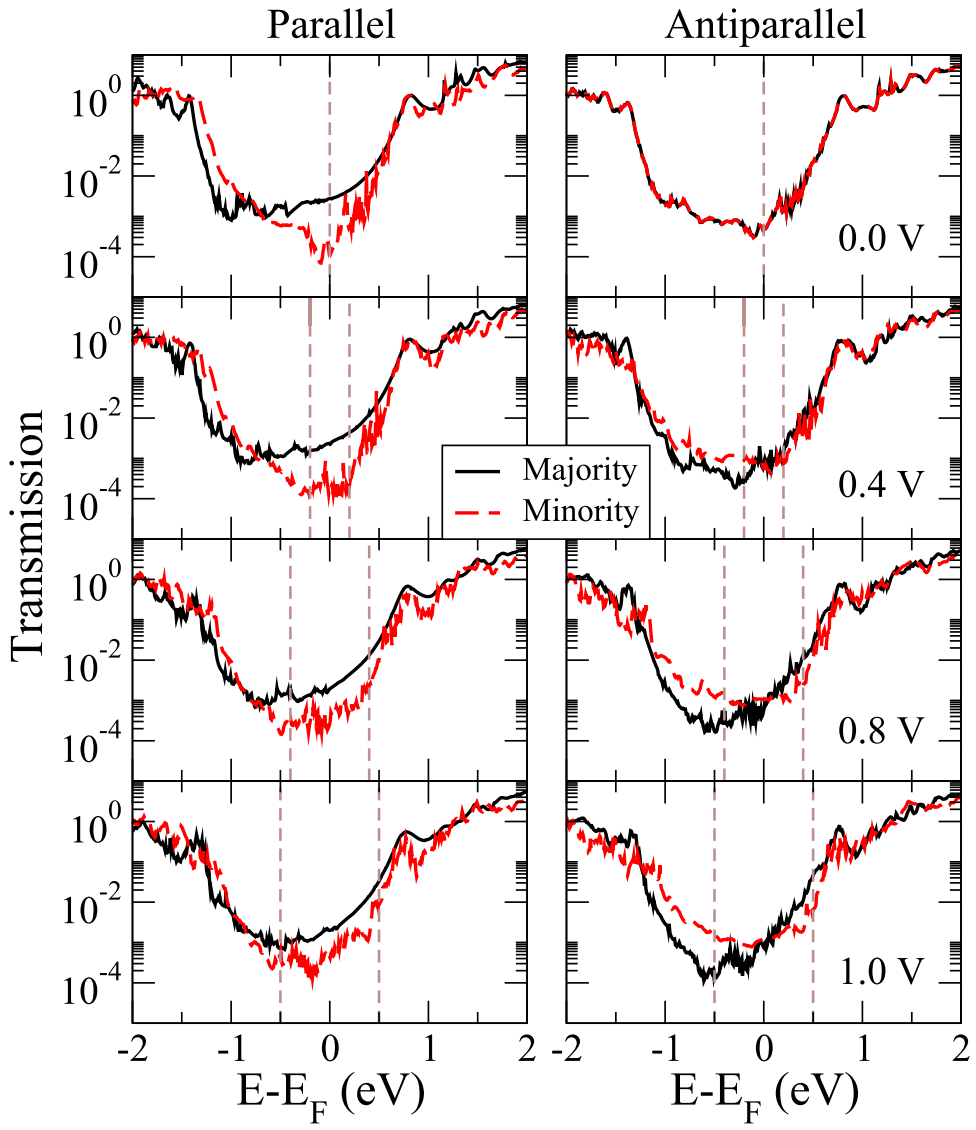

Figure 4. Zero and finite bias spin-dependent transmission coefficients for the (left panels) parallel and (right panels) antiparallel alignments of the electrodes. The vertical dashed lines enclose the bias window.

At the Fe/Si interface the situation is, however, different. The DOS of the interface Fe atoms is similar to that of bulk Fe, except for an energy downshift of about 1 eV. This reduces drastically the contribution of the majority channel at E_F, so that the DOS becomes completely dominated by the minority spin states, which are highly localized and do not contribute to the conduction. The minority spin DOS presents a relatively sharp peak just above E_F. In the case of the Si interfacial atoms the native bandgap disappears and the DOS acquires a small spin-polarization. This is the result of the Si/Fe hybridization at the interface, which indicates a strong electronic coupling between the SiNW and electrodes. Otherwise the DOS of the interfacial Si atoms is relatively featureless with the exception of a peak in the majority channel at 1.5 eV below E_F, which mirrors that of bulk Fe, and again is due to strong hybridization.

In order to characterize the entire MTJ, in figure 3 we present the spin-dependent total DOS and transmission coefficients for the two possible relative orientations of the electrodes' magnetizations, namely parallel and antiparallel, respectively. In this case the DOS appears as a superposition of the DOSs of the SiNW and Fe electrodes. It is spin-polarized for the parallel configuration but not for the antiparallel configuration, since the device is almost perfectly symmetric. Turning our attention to the transmission, as expected, there is a large drop in $T^{\sigma}(E)$ for an energy window of approximately 2 eV around E_F, which approximately corresponds to the SiNW bandgap. This means that our device operates in the tunneling regime, with the Fermi level of the electrodes positioned approximately at mid-gap in the SiNW. If one looks at the parallel configuration, it is possible to note that at E_F the transmission of the majority channel is approximately one order of magnitude larger than that of the minority channel. Since $T^{\sigma}(E)$ for both spins in the antiparallel configuration is

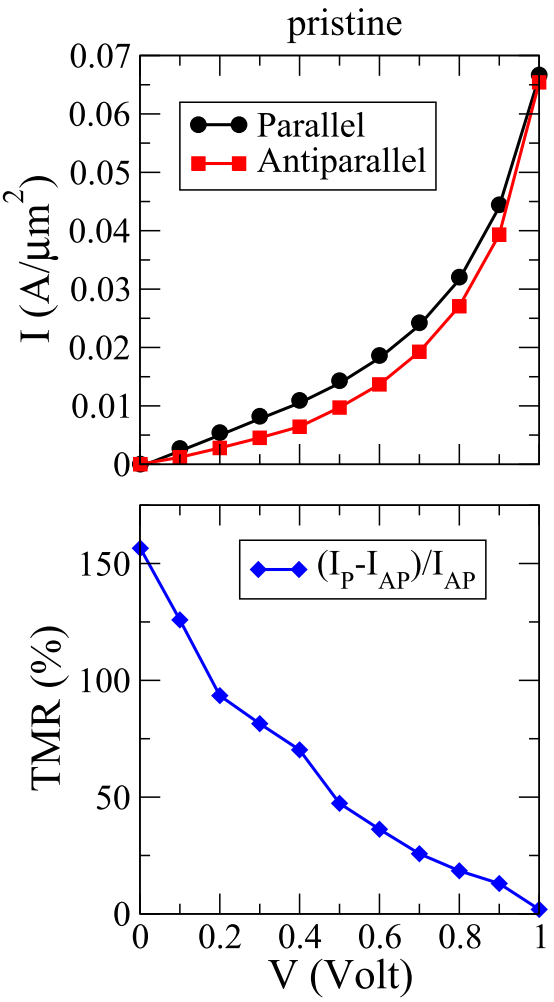

Figure 5. Current–voltage, *I–V*, characteristics for both the parallel and antiparallel alignments of the electrodes (upper panel) and TMR ratio as a function of the applied bias (lower panel). Here we show only results for positive bias, since for this symmetric junction we have $I(V) = -I(-V)$.

approximately a convolution of the different spin transmissions in the parallel configuration, a TMR has to be expected.

Since the nanowire breaks the translational invariance of the electrodes it is not possible to analyze our data by using the symmetry filtering argument valid for perfectly epitaxial junctions [7, 8]. However, the lateral confinement associated with the SiNW suggests that only electrons with small transverse wave-vector will be transmitted efficiently across the nanowire [39]. These are more abundant for the majority band, since there is a significant contribution to the DOS at E_F from states with *s* character.

The magnetoresistance is also shown in figure 3 (lower panel), obtained as the linear response limit of equation (3), i.e., by replacing the current with the total transmission coefficient. Clearly, the linear response limit is valid only for $E = E_F$, but here we present the TMR as a function of E, i.e., for a range of possible positions of E_F. We find an appreciable TMR ratio only within the gap region, in particular for energies between -0.5 and 0.5 eV, with a peak of about 200% at E_F.

We now analyze the finite bias results, obtained up to 1 V (in steps of 0.1 V), i.e., for voltages low enough to keep the junction in the tunneling regime. In figure 4 we present the spin-dependent transmission coefficient at zero and positive applied bias for both spin configurations. Since the current is essentially the integral of the bias and energy-dependent transmission coefficient over the bias window (see equation (2)) we mark the bias window in the figure with vertical lines. In a tunnel junction the electrostatic potential drops approximately linearly within the insulator, meaning that the only effect of the bias is that of shifting rigidly the DOS of the two electrodes with respect to each other by an energy eV. Furthermore, since the junction under investigation is symmetric, this shift is symmetric with respect to the common E_F established at $V = 0$. These two facts help us in analyzing figure 4.

In general, we note that the transmission coefficient remains small for all spin directions and configurations at any bias in the energy interval -1 to 1 eV. This demonstrates the symmetric potential drop across the junction.

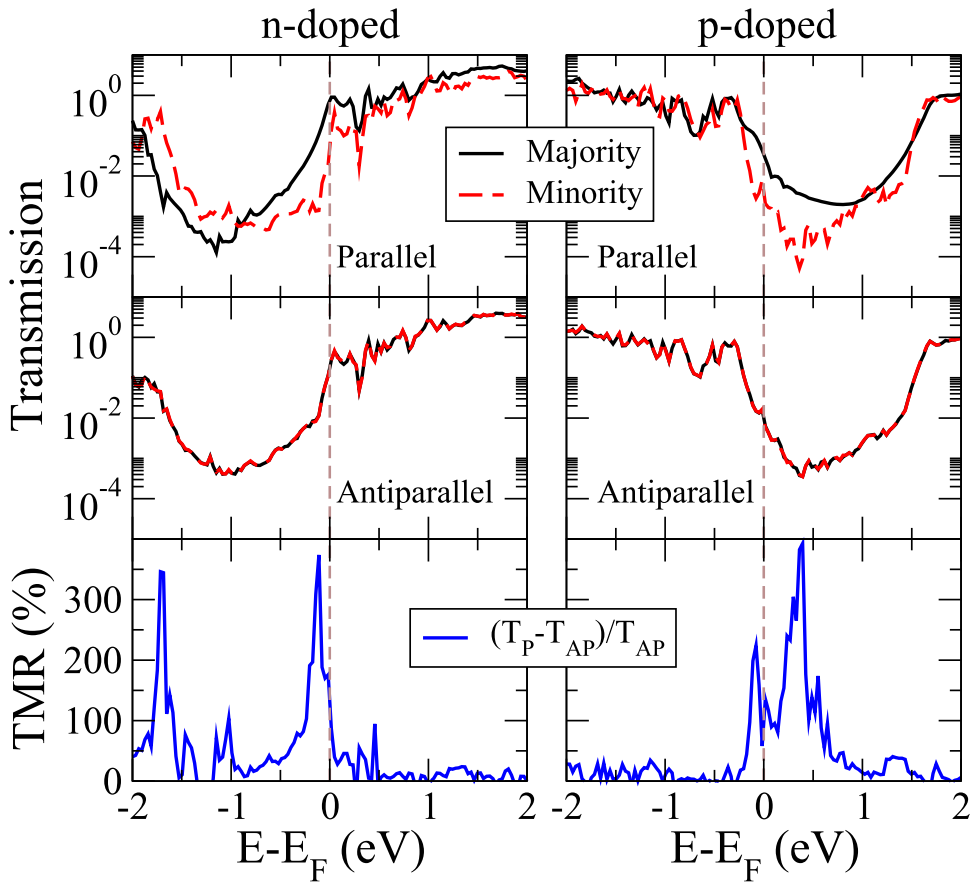

Figure 6. The upper and middle panels corresponds, respectively, to the parallel and antiparallel spin dependent transmission coefficients for a doped SiNW-MTJ, in the case of (left) *n* and (right) *p* doping. The lower panels are the TMR ratios as functions of energy.

In the parallel configuration $T^{\sigma}(E)$ is little affected by the bias for the majority spins, while for the minority spins it undergoes small modifications. Namely, the low-transmission region, which is present for energies in the interval $[-0.5, 0.5]$ eV at $V = 0$, starts spreading over a wider energy range as the bias is applied. This is the result of the relative energy shift of the band structures at the two electrodes. As a consequence, the transmission for the majority spin channel remains lower than that for the minority spin channel at all energies in the gap for any bias. In contrast, in the antiparallel case the transmission spin degeneracy, which is present at zero bias, is lifted as the bias is applied and $T^{\sigma}(E)$ becomes different for the two spin channels (note that majority and minority here refer to the magnetization orientation of the left-hand side electrode). This is due to the inversion symmetry breaking induced by the external bias. Interestingly, for the largest applied bias investigated the transmission coefficient of the majority (minority) spins in the antiparallel configuration resembles closely that of the minority (majority) spins in the parallel configuration. Since the total current determines the TMR, we expect that it will be reduced as the bias increases.

The current–voltage, *I*–*V*, characteristics and the TMR ratio as function of the bias are presented in figure 5. As expected from the small bias dependence of the transmission coefficients the *I*–*V* characteristics are rather smooth for both the parallel and the antiparallel configurations. In general they are both defined by a relatively shallow slope for voltages smaller than 0.7 V and then by a rapid increase in the current for $V > 0.7$ V. Such a rapid slope for higher voltages is due to the fact that the upper edge of the bias window starts approaching the SiNW conductance band and therefore the transmission rapidly increases (see figure 4 for $V = 0.8$ V and $V = 1$ V). A second feature of the *I*–*V* characteristics is that for high voltages the current for the parallel configuration becomes similar to that of the antiparallel configuration, as expected from the observed dependence of the transmission coefficient as a function of the bias for the two configurations. As a consequence, the TMR is high at low bias (approximately 150% for $V = 0$), halves its value for $V \sim 0.35$ V and vanishes almost entirely at 1 V. This bias dependence of the TMR is similar to that found for the Fe/MgO/Fe junction, although in that case the absolute value of the TMR is significantly larger [40].

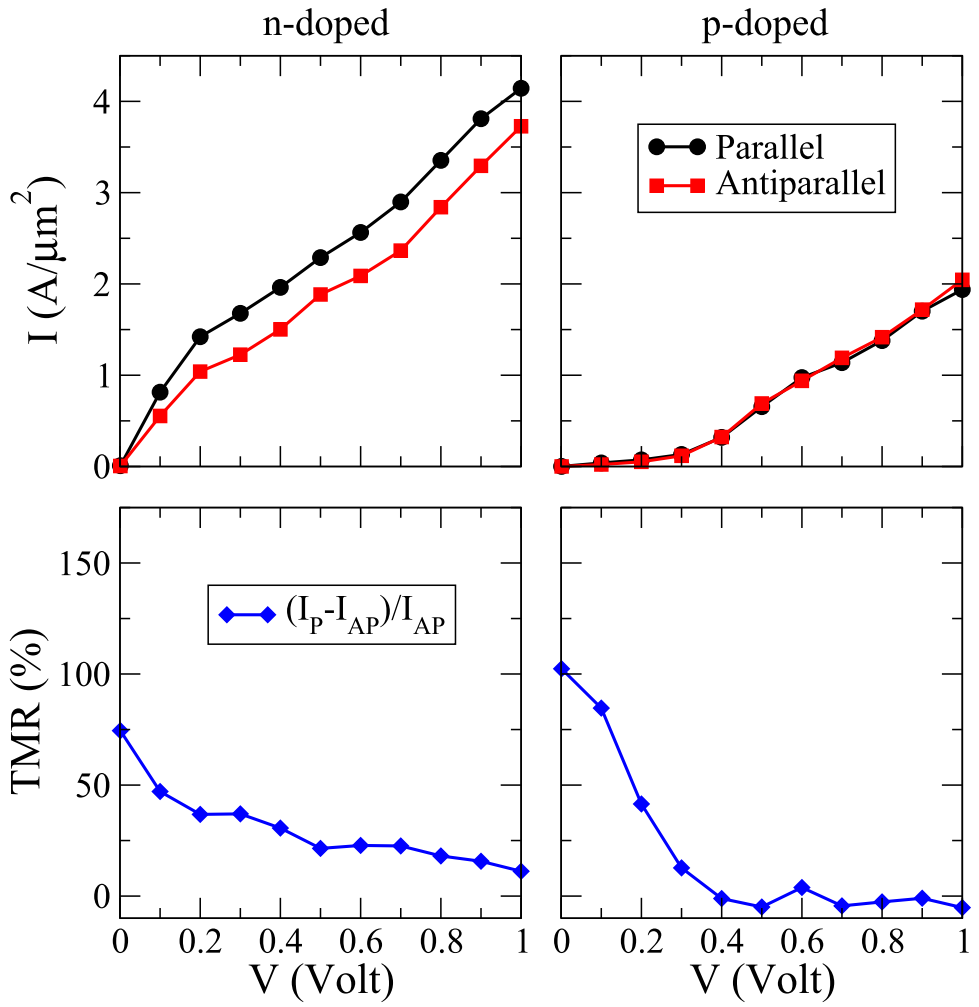

Figure 7. Current–voltage, *I–V*, characteristics and TMR ratio as a function of the bias, for the (left) *n* and (right) *p*-doped SiNW-MTJ.

3.2. Effect of doping

We finally move to studying the effect of doping on the magneto transport properties. P and B atoms are, respectively, used to obtain *n* and *p* doping in the SiNWs. These ions are known to behave as shallow impurities in bulk silicon, and can be easily ionized to create free carriers at the band edges approaching the metallic regime [41]. The doping concentration considered is about 1.8%, which corresponds to two dopant atoms in the entire SiNW. We include both dopant atoms at edge positions, in alternate unit cells along the nanowire, having equivalent distance to the closest electrode. Thus the junction remains symmetric also in this case. We place the dopants at edge positions of the nanowire, since previous studies have reported lowest formation and segregation energies for these positions [31, 32].

In figure 6 we present the zero bias spin-dependent transmission coefficients for *n* and *p* doped SiNW-MTJs, for both the parallel and antiparallel configurations of the electrodes. The TMR as a function of energy is also plotted. In general, the effect of doping is that of simply re-positioning E_F from the middle of the SiNW band gap closer to one of the band edges. As a consequence, the $T^{\sigma}(E)$ curves simply shift rigidly in energy with respect to E_F, but maintain a shape similar to that of the neutral case. The shift is more evident in the case of *n* doping, for which E_F enters the conduction band completely, while for *p* doping the transmission at E_F is still tunneling-like.

Since the maximum contrast in transmission for different spins is found in the full tunneling regime, i.e., when E_F of the electrodes is placed close to mid-gap, it is expected that doping will reduce the TMR. This is indeed the case at zero bias. The TMR as a function of energy (see figure 6 lower panels) still presents a peak with values in the region of 300%, but this peak is shifted to higher energies for *p* doping and to lower energies for *n* doping. In both cases the low bias TMR is then smaller than that calculated for the neutral case.

Finally, in figure 7 we plot the *I–V* characteristics and the TMR ratio as a function of the bias for voltages up to 1 V, for the *n* and *p*-doped SiNWs. This time the current appears to be approximately linear with the bias, indicating that the dominant transport mechanism is no longer tunneling but direct injection into one of the SiNW extremal bands. The linear behavior is more evident for *n* doping, since, as note before, E_F is located

essentially at the conduction band edge. In contrast, for the *p* doping tunneling is still the dominant mechanism for voltages up to 0.4 V where direct spin injection into the valence band becomes dominant. The TMR as a function of the bias reflects the *I–V* characteristics, namely, the TMR is substantial as long as the transport is tunneling-like and then drops drastically. Thus, for *p* doping we have an abrupt collapse of the TMR at 0.4 V, while for *n* doping the TMR is small across the entire voltage range investigated.

4. Conclusions

We have systematically studied the TMR of pristine and doped SiNW-MTJs sandwiched between Fe electrodes. The developed knowledge is essential for the design of iNW-based magnetic nanodevices. The pristine (undoped) system shows a high TMR ratio of ∼200% at low bias, and the current through the nanowire flows in the tunneling regime. While the current increases rapidly with the bias, the TMR decreases and is suppressed at about 1 V. For *n* and *p* doped SiNWs the *I–V* characteristic is metallic-like, showing an approximately linear dependance of the current on the bias. The onset of the linear *I–V* characteristics depends on the doping condition, i.e., on the position of E_F of the electrodes with respect to the SiNW band edges. The TMR remains strong only when the current is tunneling-like, meaning that it is generally smaller than that in the neutral situation and decays fast with the bias.

Acknowledgments

The research reported in this publication was supported by funding from King Abdullah University of Science and Technology (KAUST). The authors wish to acknowledge the Trinity Centre for High Performance Computing (TCHPC) for the provision of computational facilities and supports. SS acknowledges funding from the Science Foundation of Ireland (grant 14/IA/2624).

References

[1] Parkin S, Jiang X, Kaiser C, Panchula A, Roche K and Samant M 2003 *Proc. IEEE* **91** 661
[2] Moodera J S, Kinder L R, Wong T M and Meservey R 1995 *Phys. Rev. Lett.* **74** 3273
[3] Julliere M 1975 *Phys. Lett.* A **54** 225
[4] Slonczewski J C 1989 *Phys. Rev.* B **39** 6995
[5] Miyazaki T and Tezuka N 1995 *J. Magn. Magn. Mater.* **139** L231
[6] Coey J M D and Sanvito S 2004 *J. Phys. D: Appl. Phys.* **37** 988
[7] Butler W H, Zhang X-G, Schulthess T C and Maclaren J M 2001 *Phys. Rev.* B **63** 054416
[8] Mathon J and Umerski A 2001 *Phys. Rev.* B **63** 220403
[9] Parkin S S P, Kaiser C, Panchula A, Rice P M, Hughes B, Samant M and Yang S-H 2004 *Nat. Mater.* **3** 862
[10] Yuasa S, Nagahama T, Fukushima A, Suzuki Y and Ando K 2004 *Nat. Mater.* **3** 868
[11] Garcia V *et al* 2010 *Science* **327** 1106
[12] Caffrey N M, Archer T, Rungger I and Sanvito S 2011 *Phys. Rev.* B **83** 125409
[13] Pantel D, Goetze S, Hesse D and Alexe M 2012 *Nat. Mater.* **11** 289
[14] Asa M, Baldrati L, Rinaldi C, Bertoli S, Radaelli G, Cantoni M and Bertacco R 2015 *J. Phys.: Condens. Matter* **27** 504004
[15] Miao G-X and Moodera J S 2012 *Phys. Rev.* B **85** 144424
[16] Miao G-X and Moodera J S 2015 *Phys. Chem. Chem. Phys.* **17** 751
[17] Karpan V M, Giovannetti G, Khomyakov P A, Talanana M, Starikov A A, Zwierzycki M, van den Brink J, Brocks G and Kelly P J 2007 *Phys. Rev. Lett.* **99** 176602
[18] Faleev S V, Parkin S S P and Mryasov O N 2015 *Phys. Rev.* B **92** 235118
[19] Burkov A A and Hawthorn D G 2010 *Phys. Rev. Lett.* **105** 066802
[20] Kim T, Chamberlin R V and Bird J P 2013 *Nano Lett.* **13** 1106
[21] Tyryshkin A M *et al* 2012 *Nat. Mater.* **11** 143
[22] Cui Y and Lieber C M 2001 *Science* **291** 851
[23] Hayden O, Agarwal R and Lieber C M 2006 *Nat. Mater.* **5** 352
[24] Kelzenberg M D, Boettcher S W, Petykiewicz J A, Turner-Evans D B, Putnam M C, Warren E L, Spurgeon J M, Briggs R M, Lewis N S and Aatwater H A 2010 *Nat. Mater.* **9** 239
[25] Pan J, Zhou T, Jiang Z and Zhong Z 2013 *Appl. Phys. Lett.* **102** 183108
[26] Montes E, Gkionis K, Rungger I, Sanvito S and Schwingenschlögl U 2013 *Phys. Rev.* B **88** 235411
[27] Markussen T, Rurali R, Jauho A-P and Brandbyge M 2007 *Phys. Rev. Lett.* **99** 076803
[28] Marks L D 1994 *Rep. Prog. Phys.* **57** 603
[29] Zhao Y and Yakobson B I 2003 *Phys. Rev. Lett.* **91** 035501
[30] Ng M F, Zhou L, Yang S W, Sim L Y, Tan V B C and Wu P 2007 *Phys. Rev.* B **76** 155435
[31] Peelaers H, Partoens B and Peeters F M 2006 *Nano Lett.* **6** 2781
[32] Leao C R, Fazzio A and da Silva A J R 2008 *Nano Lett.* **8** 1866
[33] Soler J M, Artacho E, Gale J D, García A, Junquera J, Orjedón P and Sánchez-Portal D 2002 *J. Phys.: Condens. Matter* **14** 2745
[34] Troullier N and Martins J L 1991 *Phys. Rev.* B **43** 1993
[35] Perdew P, Burke K and Ernzerhof M 1996 *Phys. Rev. Lett.* **77** 3865
[36] Rocha A R, García-Suarez V M, Báiley S, Lambert C, Ferrer J and Sanvito S 2005 *Nat. Mater.* **4** 335

[37] Rocha A R, García-Suarez V M, Báiley S, Lambert C, Ferrer J and Sanvito S 2006 *Phys. Rev.* B **73** 085414
[38] Rungger I and Sanvito S 2008 *Phys. Rev.* B **78** 035407
[39] Tersoff J 1999 *Appl. Phys. Lett.* **74** 2122
[40] Rungger I, Mryasov O and Sanvito S 2009 *Phys. Rev.* B **79** 094414
[41] Cui Y, Duan X, Hu J and Lieber M 2000 *J. Phys. Chem.* B **104** 5213